JOURNAL OF MOLECULAR SPECTROSCOPY **180,** 414–422 (1996)
ARTICLE NO. 0265

Fourier Transform Infrared Emission Spectroscopy of the $b^1\Pi - a^1\Sigma^+$ System of BN

R. S. Ram and P. F. Bernath[1]

Department of Chemistry, University of Arizona, Tucson, Arizona 85721

Received May 22, 1996; in revised form August 1, 1996

The emission spectrum of BN has been investigated in the 1800–9000 cm^{-1} region using a Fourier transform spectrometer. BN was formed in a microwave discharge of He with a trace of BCl_3 and N_2. The bands observed in the 3000–7800 cm^{-1} interval have been assigned as the $b^1\Pi - a^1\Sigma^+$ transition, with the 0–0 band at 3513.99040(43) cm^{-1}. This transition is analogous to the $A^1\Pi_u - X^1\Sigma_g^+$ (Phillips) system of the isoelectronic C_2 molecule. The rotational analysis of the 0–0, 1–1, 1–0, 2–1, 3–2, 2–0, 3–1, 4–2, and 4–1 bands has been obtained and the molecular constants for the $b^1\Pi$ and $a^1\Sigma^+$ states have been determined. A local perturbation has been observed in the $v = 1$ vibrational level of the $b^1\Pi$ state near $J = 18$ caused by the interaction with the $v = 3$ vibrational level of the $a^1\Sigma^+$ state. The principal equilibrium constants for the $a^1\Sigma^+$ state are: $\omega_e = 1705.4032(11)$ cm^{-1}, $\omega_e x_e = 10.55338(52)$ cm^{-1}, $B_e = 1.683771(10)$, $\alpha_e = 0.013857(16)$ cm^{-1}, and $r_e = 1.2745081(37)$ Å. Although the $b^1\Pi - a^1\Sigma^+$ transition has recently been seen in emission from boron nitride trapped in solid neon matrices [*J. Chem. Phys.* **104,** 3143–3146 (1996)], our work represents the first observation of this transition of BN in the gas phase.

INTRODUCTION

BN is a ceramic material that can be formed at high temperatures by the reaction of boron atoms with N_2 or NH_3 and is of substantial chemical and industrial importance. Solid BN is isoelectronic to carbon and exists in several allotropic forms including the graphite-like α-BN and the diamond-like β-BN. The isoelectronic C_2 molecule has been studied in great detail because of its importance in combustion and astrophysics (*1*). Many electronic transitions of C_2 have been identified from the infrared to the vacuum ultraviolet region of the spectrum (*1, 2*). In contrast only a few electronic transitions are known for BN.

The BN molecule was first observed by Douglas and Herzberg (*3*) who reported the analysis of a $^3\Pi_i - {}^3\Pi_i$ transition near 28 000 cm^{-1}. In addition, they also observed three weaker bands at 34 499, 32 817, and 30 963 cm^{-1} which were left unassigned. From the appearance of these bands they concluded that they probably involved singlet electronic states. The $^3\Pi_i - {}^3\Pi_i$ transition was later reinvestigated by Bredohl *et al.* (*4*) and a new transition of BN was observed by Verma (*5*), probably between two exited states. In a separate publication Bredohl *et al.* (*6*) provided a rotational analysis of the singlet bands initially reported by Douglas and Herzberg (*3*). The bands with *R* heads at 32 817 and 34 499 cm^{-1} were assigned as the 0–0 and 1–0 bands of the $e^1\Sigma^+ - a^1\Sigma^+$ transition and the band at 30 963 cm^{-1} was identified as the 0–0 band of the $e^1\Sigma^+ - b^1\Pi$ transition. This analysis implied that the spacing between the $a^1\Sigma^+$ and $b^1\Pi$ states was 1831 cm^{-1}. They also determined an approximate value for the lower $a^1\Sigma^+$ state $\Delta G(1/2)$ vibrational interval of 1712 cm^{-1}.

The ground state of BN has been well established as a $^3\Pi$ state. Thrush (*7*) studied the molecule in a time-resolved experiment in which he observed the $^3\Pi - {}^3\Pi$ absorption bands but not the singlet bands suggesting a $^3\Pi$ ground state, in contrast to the $^1\Sigma^+$ ground state for the isoelectronic C_2 molecule. Mosher and Fosch (*8*) also observed the $A^3\Pi - X^3\Pi$ transition, analogous to the Swan system of C_2, in absorption after trapping the BN molecule in a neon matrix.

There are a number of ab initio calculations available for the spectroscopic properties of BN (*9–24*). These studies predict a $^3\Pi$ ground state. In recent ab initio work Martin *et al.* (*22*) studied the spectroscopic properties of the lowest lying $^3\Pi$ and $^1\Sigma^+$ states using large basis sets and extensive electron correlation. These calculations support the ground state assignment as $^3\Pi$ and predict that the next excited state, $a^1\Sigma^+$, lies at 381 ± 100 cm^{-1} above the ground state and that the $a^1\Sigma^+$ state has a vibrational interval $\Delta G(1/2) = 1664$ cm^{-1}. From this result they concluded that the vibrational assignments of Bredohl *et al.* (*6*) must be in error since their $a^1\Sigma^+$ vibrational interval was about 50 cm^{-1} larger than the predicted value. In an even more extensive calculation Bauschlicher and Partridge (*24*) lowered the $a^1\Sigma^+ - X^3\Pi$ interval to 180 ± 110 cm^{-1} with a $b^1\Pi - a^1\Sigma^+$ spacing of 3562 cm^{-1} and $\Delta G(1/2) = 1655$ cm^{-1} for the $a^1\Sigma^+$ state. These predictions are also at variance with the measurements of Bredohl *et al.* (*6*). In a different study Mawhinney *et al.* (*23*) performed a MRDCI ab initio study

[1] Also at Department of Chemistry, University of Waterloo, Waterloo, Ontario, Canada N2L 3G1.

0022-2852/96 $18.00

of BN^- and BN and suggested that the location of the states of BN could be experimentally determined via photodetachment. The $b^1\Pi - a^1\Sigma^+$ separation predicted in this study is 0.43 ± 0.03 eV (3470 ± 200 cm^{-1}) with the $a^1\Sigma^+$ state lying at 0.03 ± 0.02 eV (241 ± 160 cm^{-1}) above the ground state.

The recent matrix work of Lorenz *et al.* (*25*) has cleared up much of the controversy concerning the spectroscopic properties of the low-lying states of BN. In this work Lorenz *et al.* (*25*) used laser vaporization to deposit BN in a solid neon matrix. Laser excitation in the ultraviolet bands of BN resulted in near infrared emission spectra. From this study they located the positions of $a^1\Sigma^+$, $b^1\Pi$, $A^3\Sigma^+$, and $B^3\Sigma^-$ states and determined the vibrational constants for these states. This study places the $a^1\Sigma^+$ state between 15 and 182 cm^{-1} above the ground $X^3\Pi$ state, has a $b^1\Pi - a^1\Sigma^+$ T_{00} interval of 3561.6 cm^{-1}, and provides the $a^1\Sigma^+$ state $\Delta G(1/2)$ of 1681.1 cm^{-1}. The results of this work are in excellent agreement with the recent theoretical predictions (*22–24*).

In the present work we have observed the high resolution gas phase spectra of BN in the 1800–9000 cm^{-1} region and have identified a $^1\Pi - {}^1\Sigma^+$ transition with a 0–0 band at 3514 cm^{-1}. This observation is consistent with the neon matrix observations of Lorenz *et al.* (*25*) and recent the theoretical predictions (*22–24*). In this paper we report the rotational analysis of nine bands of the $b^1\Pi - a^1\Sigma^+$ transition involving the $v' = 0-4$ and the $v'' = 0-2$ vibrational levels.

EXPERIMENTAL

The infrared bands of BN were produced in an electrodeless microwave discharge through a flowing mixture of 1.9 Torr of He and traces of N_2 and BCl_3. The discharge tube was made of quartz and had an outside diameter of 12 mm. The emission from the lamp was sent directly into the entrance aperture of the 1-m Fourier transform spectrometer associated with the McMath–Pierce telescope of the National Solar Observatory. The spectrometer was equipped with a CaF_2 beam splitter and liquid nitrogen cooled InSb detectors. The use of a Si filter limited the observation of the spectra to the 1800–9000 cm^{-1} spectral region. A total of 10 scans were coadded in about 70 min at an instrumental resolution of 0.02 cm^{-1} (1/2L).

In addition to BN bands this spectrum also contained numerous lines of N_2, the vibration–rotation bands of HCl, and many atomic lines of the He, N, and B atoms. The spectra were calibrated using the measurements of the HCl vibration–rotation lines made by LeBlanc *et al.* (*26*). Their wavenumber scale was calibrated to better than ±0.001 cm^{-1} (*26*). The BN lines have a typical width of 0.032 cm^{-1} and have been observed with a maximum signal-to-noise ratio of 30:1. The measurements of the strong and unblended BN lines are therefore expected to be accurate to ±0.001 cm^{-1}.

OBSERVATION AND ANALYSIS

The spectra were measured using a program called PC-DECOMP developed by J. Brault. The peak positions were determined by fitting a Voigt line shape function to each spectral feature and the branches were sorted using a color Loomis–Wood program running on a PC computer.

The BN bands are located in the 3000–7900 cm^{-1} region. All of the observed bands belong to a single $^1\Pi - {}^1\Sigma^+$ transition with the 0–0 band at 3514 cm^{-1}. A major portion of the BN bands are overlapped by strong molecular lines from the infrared bands of N_2. Only bands in the $\Delta v = 0$ and $\Delta v = 1$ sequences are free from overlapping by N_2. The 1–0 band is the most intense band and we also identified the 2–1 and 3–2 bands in the $\Delta v = 1$ sequences. In the $\Delta v = 0$ sequence we found the 0–0 and 1–1 bands. The 0–1 band is located near 1850 cm^{-1} which is at the sharp cutoff in the InSb detector response and therefore could not be identified. The rotational analysis of the 0–0, 1–1, 1–0, 2–1, and 3–2 bands provided enough data to predict and search for the bands in the $\Delta v = 2$, 3, and 4 sequences. The 2–0, 3–1, 4–2, and 4–1 bands were identified using these predictions in spite of overlapping from strong N_2 bands. The search for the bands having $v'' = 3$ was unsuccessful because of the very weak intensity of these bands.

Boron has two isotopes ^{10}B and ^{11}B with natural abundances of 20 and 80%, respectively. The ^{10}BN bands are expected to appear with the 25% of the intensity of the ^{11}BN bands and we were able to identify ^{10}BN lines only in the 0–0 and 1–0 bands. A compressed portion of the 1–0 band is presented in Fig. 1 with the *R* heads of both isotopomers marked.

Each band of the $b^1\Pi - a^1\Sigma^+$ transition consists of a single *R*, a single *P*, and a single *Q* branch with no Λ doubling, as expected. The observation of the first lines $R(0)$, $Q(1)$, and $P(2)$ in the stronger bands confirms this assignment. The *R* and *P* branches appear with almost the same intensity and the *Q* branch is the most intense branch. The 0–0 band is free from perturbation and the lines up to $R(33)$, $P(36)$, and $Q(33)$ have been identified. The bands with $v' = 1$ show a perturbation at $J' = 18$ caused by the interaction between the $v'' = 3$ ($a^1\Sigma^+$) and $v' = 1$ ($b^1\Pi$) levels.

A part of the *Q* branch of the 0–0 band is provided in Fig. 2 with lines marked from both ^{10}BN and ^{11}BN. The wavenumbers and the assignment of the rotational lines in the different bands of the ^{11}BN and ^{10}BN are listed in Tables 1 and 2, respectively. The molecular constants were determined by fitting the observed line positions with the customary energy level expressions for $^1\Sigma^+$ (Eq. [1]) and $^1\Pi$ (Eq. [2]) states:

$$F_v(J) = T_v + B_v J(J+1) - D_v[J(J+1)]^2 + H_v[J(J+1)]^3 \quad [1]$$

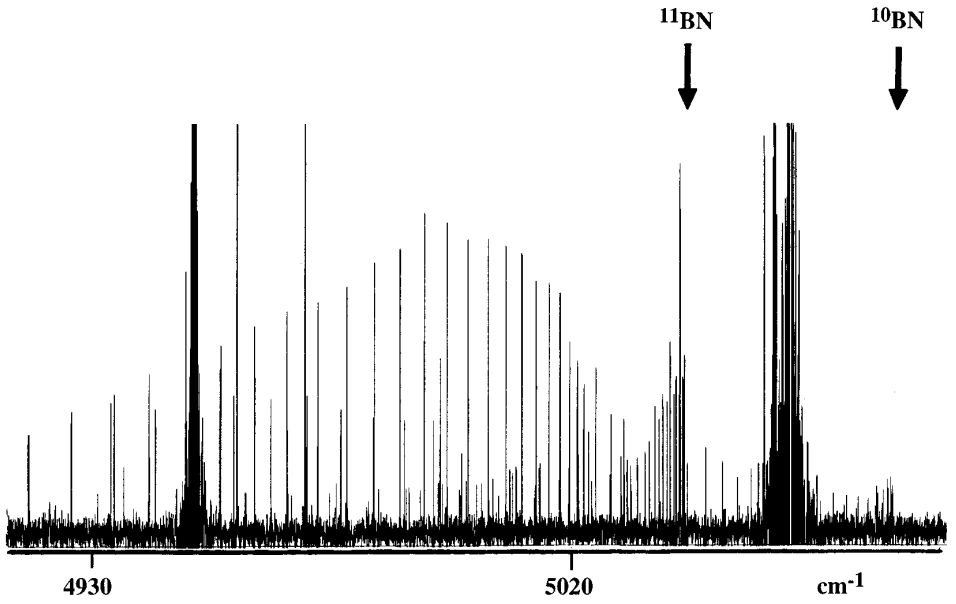

FIG. 1. A compressed portion of the 1−0 band of the $b^1\Pi-a^1\Sigma^+$ system of BN with R heads of ^{10}BN and ^{11}BN marked by arrows.

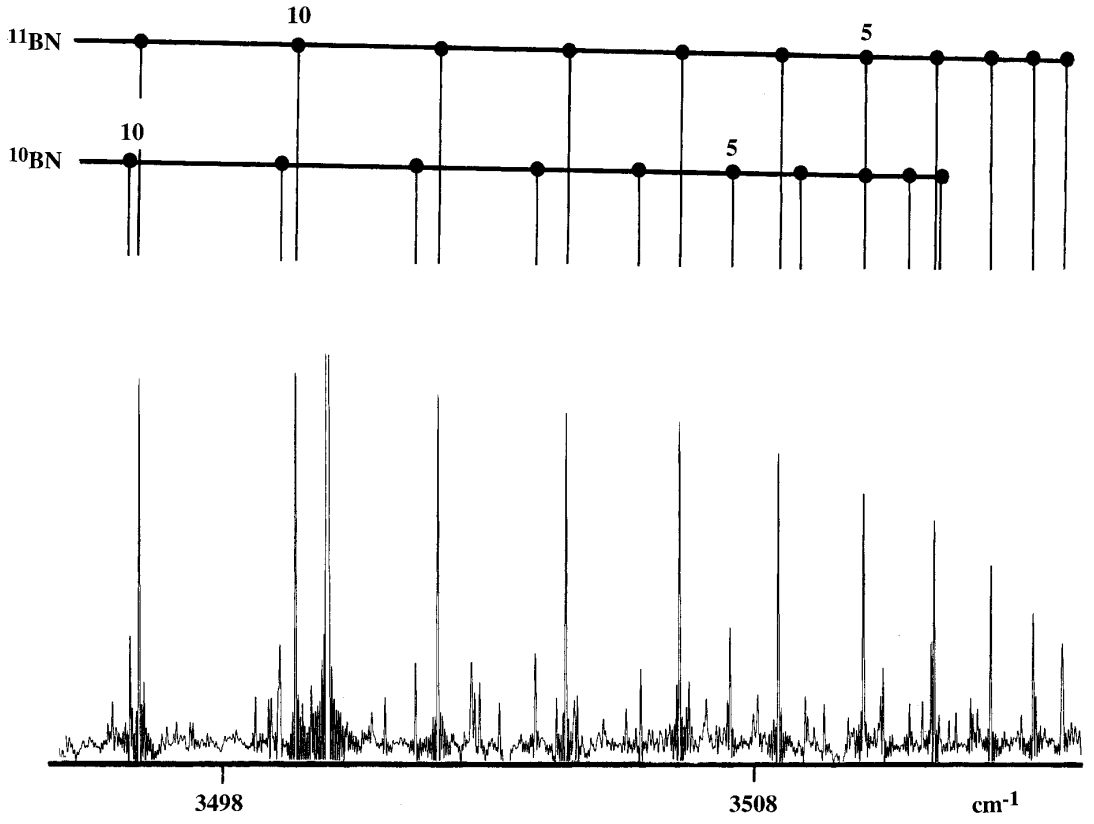

FIG. 2. An expanded portion of the 0−0 band of the $b^1\Pi-a^1\Sigma^+$ system of BN near the Q head. The assignments of some low J lines of ^{10}BN and ^{11}BN have been marked.

TABLE 1
Observed Line Positions (in cm^{-1}) of the $b^1\Pi - a^1\Sigma^+$ Bands of ^{11}BN

	0 - 0					
J	R(J)	O-C	Q(J)	O-C	P(J)	O-C
0	3517.0760	-0.0001				
1	3519.8940	0.0000	3513.7384	0.0152		
2	3522.4444	0.0007	3513.1883	-0.0005	3507.0088	-0.0073
3	3524.7258	0.0005	3512.3869	-0.0003	3503.1263	-0.0014
4	3526.7375	-0.0012	3511.3179	-0.0005	3498.9667	-0.0054
5	3528.4849	0.0014	3509.9828	0.0005	3494.5484	-0.0009
6	3529.9592	-0.0004	3508.3782	-0.0007	3489.8591	-0.0003
7	3531.1682	0.0015	3506.5072	-0.0008	3484.9027	0.0001
8	3532.1068	0.0020	3504.3687	-0.0011	3479.6787	-0.0003
9	3532.7698	-0.0038	3501.9633	-0.0009	3474.1888	0.0001
10	3533.1725	-0.0004	3499.2900	-0.0009	3468.4325	0.0008
11	3533.3032	0.0006	3496.3488	-0.0012	3462.4089	0.0007
12	3533.1643	0.0020	3493.1400	-0.0015	3456.1182	0.0000
13	3532.7554	0.0035	3489.6665	0.0014	3449.5615	-0.0004
14	3532.0732	0.0020	3485.9196	-0.0013	3442.7408	0.0014
15	3531.1202	0.0002	3481.9074	-0.0014	3435.6519	0.0013
16	3529.9003	0.0022	3477.6272	-0.0016	3428.2969	0.0010
17	3528.4060	0.0007	3473.0795	-0.0011	3420.6760	0.0007
18	3526.6426	0.0013	3468.2629	-0.0014	3412.7903	0.0015
19	3524.6063	0.0002	3463.1789	-0.0009	3404.6374	0.0008
20	3522.3000	0.0005	3457.8258	-0.0013	3396.2197	0.0009
21	3519.7214	0.0001	3452.2062	0.0001	3387.5376	0.0020
22	3516.8693	-0.0020			3378.5877	0.0005
23	3513.7384	-0.0111	3440.1594	0.0001	3369.3745	0.0008
24	3510.3558	0.0001	3433.7352	0.0018	3359.8946	-0.0007
25	3506.6874	-0.0026	3427.0411	0.0018	3350.1521	-0.0001
26	3502.7531	0.0010	3420.0792	0.0023	3340.1444	-0.0004
27	3498.5394	-0.0027	3412.8466	0.0001	3329.8725	-0.0008
28	3494.0643	0.0043	3405.3483	0.0003	3319.3344	-0.0034
29	3489.3047	-0.0011	3397.5839	0.0024	3308.5370	-0.0019
30	3484.2883	0.0087	3389.5500	0.0026	3297.4733	-0.0035
31	3478.9793	-0.0021	3381.2457	-0.0001	3286.1503	-0.0017
32	3473.4134	0.0019	3372.6734	-0.0035	3274.5637	-0.0012
33	3467.5736	0.0036	3363.8345	-0.0065	3262.7184	0.0023
34					3250.6025	-0.0035
35					3238.2367	0.0015
36					3225.6119	0.0074

	1 - 1						1 - 0					
J	R(J)	O-C	Q(J)	O-C	P(J)	O-C	R(J)	O-C	Q(J)	O-C	P(J)	O-C
0							5026.5326	-0.0011				
1	3345.0208	-0.0006	3338.9176	0.0039			5029.2893	0.0014	5023.1810	0.0008		
2	3347.5385	0.0030	3338.3721	-0.0020			5031.7423	0.0003	5022.5817	0.0011	5016.4769	0.0031
3	3349.7829	0.0033	3337.5655	0.0007	3328.4141	0.0090	5033.8958	-0.0003	5021.6891	0.0078	5012.5187	-0.0030
4	3351.7524	-0.0011	3336.4846	-0.0011	3324.2681	-0.0058	5035.7479	-0.0021	5020.4836	0.0014	5008.2704	0.0000
5	3353.4565	-0.0007	3335.1398	0.0030			5037.3016	-0.0019	5018.9848	0.0016	5003.7173	-0.0027
6					3315.1983	-0.0065	5038.5547	-0.0016	5017.1863	0.0021	4998.8689	-0.0019
7					3310.2618	-0.0054	5039.5075	-0.0008	5015.0866	0.0012	4993.7200	-0.0026
8	3356.9470	0.0022	3329.4723	0.0003	3305.0588	-0.0025	5040.1576	-0.0016	5012.6868	0.0003	4988.2741	-0.0016
9	3357.5666	0.0008	3327.0449	0.0004	3299.5822	-0.0049	5040.5097	0.0008	5009.9878	0.0002	4982.5271	-0.0031
10	3357.9202	0.0042	3324.3479	0.0006	3293.8472	0.0023	5040.5636	0.0064	5006.9891	0.0006	4976.4842	-0.0019
11	3358.0099	0.0149 *	3321.3799	-0.0006	3287.8337	-0.0010	5040.3186	0.0149 *	5003.6906	0.0014	4970.1444	0.0009
12	3357.8323	0.0294 *	3318.1436	-0.0006	3281.5606	0.0036	5039.7796	0.0313 *	5000.0892	-0.0004	4963.5085	0.0061
13	3357.4008	0.0613 *	3314.6388	0.0004	3275.0268	0.0150 *	5038.9489	0.0581 *	4996.1891	-0.0006	4956.5780	0.0150 *
14	3356.7139	0.1091 *	3310.8642	0.0009	3268.2331	0.0338 *	5037.8391	0.1083 *	4991.9897	0.0004		
15			3306.8186	-0.0001			5036.4844	0.2162 *	4987.4878	-0.0006	4941.8474	0.0579 *
16			3302.5040	-0.0008	3253.8834	0.1099 *	5034.9970	0.4942 *	4982.6868	0.0000	4934.0651	0.1096 *
17			3297.9200	-0.0017	3246.3805	0.2199 *	5033.9517	1.5175 *	4977.5828	-0.0018	4926.0386	0.2152 *
18	3350.0575	-0.8927 *	3293.0654	-0.0040	3238.7283	0.4471 *	5029.1660	-0.8964 *	4972.1807	-0.0009	4917.8863	0.4929 *
19	3348.2536	-0.6036 *	3287.9473	-0.0007	3231.6553	1.5196 *	5026.7841	-0.6029 *	4966.4773	-0.0005	4910.1893	1.5237 *
20	3345.9975	-0.4949 *	3282.5569	-0.0006			5023.9165	-0.4914 *	4960.4714	-0.0018	4898.7491	-0.8907 *
21	3343.4071	-0.4484 *	3276.8992	0.0010	3212.4415	-0.6056 *	5020.6781	-0.4468 *	4954.1658	-0.0018	4889.7141	-0.6024 *
22	3340.5274	-0.4192 *	3270.9690	-0.0009	3203.6107	-0.4937 *	5017.1153	-0.4225 *	4947.5633	0.0021	4880.2023	-0.4934 *
23	3337.3516	-0.4141 *	3264.7741	0.0013	3194.4474	-0.4491 *	5013.2307	-0.4158 *	4940.6537	0.0000	4870.3321	-0.4452 *
24			3258.3081	0.0010	3184.9977	-0.4259 *	5009.0383	-0.4123 *	4933.4453	-0.0000		
25			3251.5723	-0.0005			5004.5319	-0.4184 *	4925.9364	0.0004	4849.6332	-0.4160 *
26			3244.5712	0.0012			4999.7201	-0.4252 *	4918.1265	0.0007	4838.8292	-0.4105 *
27			3237.3004	0.0017			4994.6037	-0.4319 *	4910.0160	0.0013	4827.7197	-0.4138 *
28			3229.7530	-0.0062			4989.1752	-0.4457 *	4901.6056	0.0026	4816.3082	-0.4228 *
29			3221.9597	0.0082			4983.4425	-0.4591 *	4892.8907	-0.0001	4804.6033	-0.4290 *
30			3213.8733	-0.0025			4977.4035	-0.4739 *	4883.8780	0.0001	4792.5960	-0.4418 *
31			3205.5331	0.0011			4971.0531	-0.4954 *	4874.5639	-0.0011	4780.2879	-0.4600 *
									4864.9505	-0.0016	4767.6810	-0.4818 *

Note: Asterisks mark perturbed lines not included in the fit. See Text for details.

TABLE 1—*Continued*

	2 - 1						2 - 0					
J	R(J)	O-C	Q(J)	O-C	P(J)	O-C	R(J)	O-C	Q(J)	O-C	P(J)	O-C
0	4829.5103	-0.0004										
1	4832.2288	0.0013	4826.2028	0.0147								
2	4834.6399	-0.0008	4825.5800	-0.0032								
3	4836.7490	-0.0013	4824.6772	0.0012	4815.6045	-0.0067	6520.8702	0.0035	6508.7940	0.0015		
4	4838.5580	0.0020			4811.3782	-0.0009	6522.5565	0.0040	6507.4637	0.0010		
5	4840.0561	-0.0018	4821.9557	0.0015	4806.8451	0.0007	6523.9033	-0.0009	6505.7995	-0.0010		
6	4841.2523	-0.0033	4820.1417	0.0019	4802.0070	-0.0002	6524.9310	0.0094	6503.8090	0.0032	6485.6743	0.0011
7	4842.1459	-0.0033	4818.0230	0.0000	4796.8701	0.0022	6525.6012	-0.0034	6501.4792	0.0008	6480.3186	-0.0047
8	4842.7364	-0.0022	4815.6045	0.0006	4791.4254	-0.0012	6525.9543	0.0013	6498.8142	-0.0041	6474.6399	-0.0012
9	4843.0208	-0.0027	4812.8825	0.0000			6525.9651	-0.0015	6495.8243	-0.0013	6468.6251	-0.0015
10	4843.0046	0.0007	4809.8604	0.0015	4779.6380	-0.0006	6525.6449	-0.0002	6492.5012	0.0011	6462.2851	0.0053
11	4842.6793	-0.0005	4806.5342	0.0012	4773.2900	-0.0024	6524.9862	-0.0023			6455.5990	-0.0021
12	4842.0508	-0.0002	4802.9043	-0.0007	4766.6423	-0.0027	6523.9975	0.0011			6448.5842	-0.0062
13	4841.1178	0.0004	4798.9754	0.0005	4759.6953	-0.0013	6522.6660	-0.0027	6480.5259	-0.0002		
14	4839.8773	-0.0018	4794.7437	0.0010	4752.4443	-0.0032	6521.0045	-0.0006	6475.8704	0.0017	6433.5752	0.0017
15	4838.3352	-0.0005	4790.2094	0.0010	4744.8936	-0.0042	6519.0092	0.0038	6470.8777	-0.0004	6425.5652	-0.0022
16	4836.4879	0.0004	4785.3725	0.0002	4737.0460	-0.0018	6516.6728	0.0033	6465.5545	0.0002	6417.2296	-0.0002
17	4834.3350	0.0008	4780.2343	-0.0000	4728.8971	-0.0007			6459.8933	-0.0038	6408.5610	0.0003
18	4831.8736	-0.0024	4774.7947	0.0003	4720.4498	0.0018			6453.9060	-0.0007		
19	4829.1135	0.0010	4769.0513	-0.0015	4711.6995	0.0009			6447.5825	-0.0002		
20	4826.0434	-0.0004	4763.0085	-0.0011	4702.6511	0.0012						
21			4756.6648	0.0001	4693.3018	-0.0005			6433.9380	0.0038		
22	4818.9935	0.0026	4750.0195	0.0012	4683.6581	0.0022			6426.6085	-0.0011		
23	4815.0088	0.0022	4743.0686	-0.0020	4673.7124	0.0013			6418.9503	-0.0011		
24	4810.7224	0.0055	4735.8218	0.0004	4663.4745	0.0065			6410.9587	-0.0009		
25	4806.1209	-0.0012	4728.2711	-0.0001	4652.9273	0.0003						
26	4801.2158	-0.0061	4720.4189	-0.0007	4642.0813	-0.0071						
27	4796.0165	0.0001	4712.2683	0.0011	4630.9485	-0.0041						
28	4790.5055	-0.0002	4703.8139	0.0001	4619.5160	-0.0036						
29	4784.6885	-0.0010	4695.0576	-0.0020								
30	4778.5749	0.0067	4686.0027	-0.0020								
31			4676.6507	0.0014								
32												
33			4657.0342	-0.0030								
34			4646.7802	-0.0006								
35			4636.2250	0.0007								
36			4625.3832	0.0152								

	3 - 2						3 - 1					
J	R(J)	O-C	Q(J)	O-C	P(J)	O-C	R(J)	O-C	Q(J)	O-C	P(J)	O-C
1	4634.1324	-0.0038										
2			4627.5534	-0.0028								
3	4638.5900	-0.0021	4626.6456	-0.0021			6301.5877	-0.0006	6289.6485	0.0046		
4	4640.3660	0.0022	4625.4340	-0.0023			6303.2403	0.0092	6288.3011	-0.0024		
5	4641.8349	0.0036	4623.9257	0.0035	4608.9750	-0.0015	6304.5341	-0.0033	6286.6345	0.0064		
6			4622.1071	0.0019	4604.1677	-0.0022	6305.5065	-0.0004	6284.6199	0.0022	6271.6934	0.0110
7	4643.8480	-0.0051	4619.9869	0.0014	4599.0671	0.0064	6306.1479	0.0082	6282.2710	-0.0012	6266.6795	-0.0028
8	4644.4127	0.0056	4617.5626	-0.0006			6306.4397	0.0041	6279.5863	-0.0054	6261.3535	0.0061
9	4644.6566	0.0003	4614.8396	0.0016	4587.9345	-0.0013	6306.3931	-0.0014			6255.6766	-0.0013
10	4644.5998	-0.0010	4611.8079	-0.0025	4581.9236	0.0033	6306.0161	-0.0001	6273.2266	0.0008	6249.6729	-0.0010
11	4644.2395	-0.0008	4608.4820	0.0018	4575.6020	-0.0010	6305.2994	-0.0012	6269.5387	-0.0019	6243.3341	-0.0016
12	4643.5764	0.0016	4604.8469	-0.0007	4568.9854	0.0010	6304.2490	0.0012	6265.5218	0.0013	6236.6619	-0.0015
13	4642.6041	-0.0003	4600.9123	-0.0001	4562.0690	0.0046	6302.8585	0.0011	6261.1662	0.0007	6229.6557	-0.0015
14	4641.3283	-0.0005	4596.6770	0.0020	4554.8482	0.0048	6301.1232	-0.0064	6256.4745	-0.0013	6222.3196	0.0022
15	4639.7471	-0.0009	4592.1355	0.0002	4547.3222	0.0005			6251.4502	-0.0012	6214.6466	0.0024
16	4637.8640	0.0020	4587.2951	0.0018	4539.5017	0.0023	6296.6525	-0.0084	6246.0926	0.0004	6206.6381	0.0003
17	4635.6711	0.0005	4582.1516	0.0023	4531.3741	-0.0027			6240.3988	0.0002	6198.2988	0.0005
18	4633.1783	0.0044	4576.7034	0.0001	4522.9556	0.0014	6290.8383	-0.0028	6234.3681	-0.0023	6189.6272	0.0011
19	4630.3713	-0.0007	4570.9560	0.0007	4514.2272	-0.0047	6287.4193	-0.0050	6228.0064	-0.0014	6180.6191	-0.0023
20	4627.2725	0.0080			4505.2078	-0.0023	6283.6712	0.0016	6221.3120	0.0013		
21	4623.8562	0.0045	4558.5521	-0.0021			6279.5863	0.0095	6214.2795	0.0002	6161.6103	-0.0049
22	4620.1308	-0.0027	4551.9017	0.0005			6275.1462	0.0003	6206.9112	-0.0025	6151.6197	0.0055
23	4616.1063	-0.0034					6270.3770	0.0001	6199.2148	0.0010	6141.2823	0.0006
24							6265.2733	0.0038	6191.1758	-0.0042	6130.6197	0.0019
25									6182.8187	0.0066	6119.6204	-0.0026
26									6174.1110	0.0006		

TABLE 1—*Continued*

	4 - 2						4 - 1					
J	R(J)	O-C	Q(J)	O-C	P(J)	O-C	R(J)	O-C	Q(J)	O-C	P(J)	O-C
2	6079.2925	0.0009	6070.4268	-0.0022								
3	6081.2385	0.0009	6069.4235	0.0008					7732.4174	-0.0016		
4	6082.8462	-0.0007	6068.0817	0.0004	6056.2529	-0.0028	7745.7265	0.0123	7730.9437	-0.0048		
5	6084.1212	0.0017	6066.4044	0.0001	6051.6234	0.0014	7746.8340	0.0086	7729.1108	0.0005		
6	6085.0538	-0.0012	6064.3881	-0.0040	6046.6566	0.0036	7747.5699	0.0023	7726.9007	-0.0038	7709.1625	-0.0030
7	6085.6552	0.0017			6041.3514	0.0026	7747.9437	0.0035	7724.3325	0.0014	7703.6346	-0.0010
8	6085.9123	-0.0024	6059.3636	0.0021	6035.7080	-0.0019			7721.3914	0.0013	7697.7432	0.0048
9	6085.8389	0.0002	6056.3427	-0.0007	6029.7378	0.0016	7747.5758	-0.0010	7718.0804	-0.0011	7691.4752	0.0008
10	6085.4197	-0.0054	6052.9905	0.0006	6023.4261	-0.0018	7746.8380	-0.0025	7714.4022	-0.0032	7684.8442	0.0008
11	6084.6687	-0.0052	6049.2960	-0.0052	6016.7833	-0.0021	7745.7319	-0.0023	7710.3642	0.0026	7677.8536	0.0079
12	6083.5848	0.0000	6045.2777	0.0003	6009.8076	-0.0010	7744.2562	-0.0015	7705.9536	0.0034	7670.4774	-0.0041
13	6082.1581	0.0001	6040.9193	0.0009	6002.4994	0.0015	7742.4167	0.0057	7701.1694	-0.0020	7662.7590	0.0081
14	6080.3950	0.0020	6036.2224	-0.0018	5994.8535	0.0002	7740.1922	-0.0017	7696.0225	-0.0025	7654.6520	-0.0021
15	6078.2916	0.0015	6031.1937	-0.0012	5986.8776	0.0024	7737.6073	0.0011	7690.5115	0.0005		
16	6075.8494	0.0005	6025.8301	-0.0005	5978.5621	-0.0016	7734.6419	-0.0059	7684.6266	-0.0030		
17	6073.0713	0.0020	6020.1325	0.0012	5969.9178	-0.0011	7731.3111	-0.0076	7678.3823	0.0016		
18	6069.9454	-0.0059	6014.0972	0.0001	5960.9379	-0.0033			7671.7630	-0.0013		
19	6066.4996	0.0049	6007.7298	0.0018	5951.6323	0.0017			7664.7788	-0.0016		
20	6062.6985	-0.0009	6001.0202	-0.0038	5941.9903	0.0028			7657.4339	0.0047		
21	6058.5664	0.0010	5993.9835	-0.0018	5932.0093	-0.0026			7649.7129	0.0025		
22	6054.0895	-0.0031	5986.6110	-0.0009	5921.7029	-0.0013			7641.6280	0.0037		
23			5978.9002	-0.0036	5911.0615	-0.0030			7633.1732	0.0023		
24			5970.8605	-0.0006	5900.0918	-0.0012			7624.3467	-0.0034		
25			5962.4868	0.0028	5888.7944	0.0044			7615.1607	-0.0014		
26			5953.7720	-0.0004	5877.1566	0.0008			7605.6077	0.0010		
27			5944.7290	0.0026	5865.1924	0.0020			7595.6812	-0.0029		
28			5935.3450	-0.0011	5852.8927	-0.0014						

$$F_v(J) = T_v + B_vJ(J+1) - D_v[J(J+1)]^2 + H_v[J(J+1)]^3 \pm 1/2\{qJ(J+1) + q_D[J(J+1)]^2 + q_H[J(J+1)]^3\}. \quad [2]$$

In this fit the perturbed lines were not included although the unperturbed lower state combination differences were added. For the final fit the lines of all the bands were fitted together and the approximate standard deviation of the residuals was ± 0.0018 cm^{-1}. The molecular constants obtained for the $a^1\Sigma^+$ and $b^1\Pi$ state vibrational levels of ^{11}BN and ^{10}BN are provided in Tables 3 and 4, respectively.

DISCUSSION

Prior to the recent work of Lorenz *et al.* (*25*) only the $C^3\Pi - X^3\Pi$ transition (Fig. 3) [previously called $A^3\Pi - X^3\Pi$ (*3, 4*) and $D^3\Pi - X^3\Pi$ (*25*)] of BN was analyzed in detail (*3, 4*). We have taken this opportunity to relabel many of the low-lying states of BN on the basis of ab initio calculations (*24*) and by analogy with C_2. The work of Lorenz *et al.* (*25*) provides new spectroscopic data for $A^3\Sigma^+$, $B^3\Sigma^-$, $b^1\Pi$, and $a^1\Sigma^+$ states with the $A^3\Sigma^+$ and $B^3\Sigma^-$ states detected for the first time. Lorenz *et al.* (*25*) confirmed that there are problems with the assignments made by Bredohl *et al.* (*6*) for the singlet bands. Our work on the $b^1\Pi - a^1\Sigma^+$ transition in the gas phase is consistent with the neon matrix observations of Lorenz *et al.* (*25*).

We have checked the rotational assignments of the singlet band in the 30 000–34 000 cm^{-1} region. Bredohl *et al.* (*6*) obtained a rotational analysis for three bands with heads at 30 963, 32 817, and 34 498 cm^{-1}. The bands at 32 817 and 34 498 cm^{-1} were assigned as the 0–0 and 1–0 bands of the $e^1\Sigma^+ - a^1\Sigma^+$ (Fig. 3) while the band at 30 963 cm^{-1} was assigned as the 0–0 band of the $e^1\Sigma^+ - b^1\Pi$ transition. A fresh look at the data of these bands indicates that the 0–0 band of the $e^1\Sigma^+ - a^1\Sigma^+$ transition is in fact the 0–1 band. Bredohl *et al.*'s 1–0 band is in the right position to be the 0–0 band but some of the *R* line positions and most of the *P* line positions do not match with the predicted line positions of the 0–0 band. The *J* numbering of the observed lines near the head that do match with the predicted lines should be increased by 2. It is not surprising to find a misassignment in this band since Bredohl *et al.* (*6*) state that it is ''much weaker and strongly overlapped by BCl bands.'' Their analysis of the $e^1\Sigma^+ - b^1\Pi$ 0–0 band is correct. This reassignment places the $e^1\Sigma^+$ $v = 0$ level at 34 476.60 cm^{-1} above the $a^1\Sigma^+$ $v = 0$ state. A comprehensive energy level diagram of the low-lying states of BN is presented in Fig. 3. In this figure the positions of the as yet undetected $c^1\Delta$ and $d^1\Sigma^+$ states are taken from the calculations of Bauschlicher and Partridge (*24*).

The relative position of the $a^1\Sigma^+$ state with respect to the $X^3\Pi$ state has been estimated to be between 15 and 182

TABLE 2
Observed Line Positions (in cm^{-1}) of the $b^1\Pi - a^1\Sigma^+$ Bands of ^{10}BN

	0 - 0						1 - 0					
J	R(J)	O-C	Q(J)	O-C	P(J)	O-C	R(J)	O-C	Q(J)	O-C	P(J)	O-C
0	3514.9544	-0.0027										
1	3517.9342	0.0022	3511.4147	-0.0028								
2	3520.6269	0.0029	3510.8554	0.0023			5070.7499	-0.0009				
3	3523.0343	0.0013					5073.0137	-0.0025				
4	3525.1560	-0.0027	3508.8791	0.0012	3495.8480	0.0010	5074.9609	-0.0017			5045.9747	0.0010
5	3526.9984	-0.0024	3507.4657	-0.0011	3491.1775	-0.0012	5076.5909	0.0012			5041.1634	0.0015
6	3528.5568	-0.0023	3505.7763	0.0027	3486.2286	0.0001	5077.8994	0.0019	5055.3702	-0.0018	5036.0269	-0.0056
7	3529.8356	0.0023	3503.7996	0.0017	3480.9928	-0.0038	5078.8841	-0.0015	5053.1514	0.0029	5030.5875	0.0019
8	3530.8230	-0.0001	3501.5412	0.0013	3475.4819	-0.0011	5079.5529	-0.0010	5050.6091	0.0018	5024.8216	0.0003
9	3531.5250	-0.0033	3498.9993	-0.0002	3469.6846	-0.0031	5079.8987	-0.0033	5047.7477	-0.0006	5018.7413	0.0014
10			3496.1777	0.0012	3463.6104	-0.0003	5079.9281	-0.0018	5044.5729	0.0015	5012.3393	-0.0021
11			3493.0742	0.0033	3457.2486	-0.0036	5079.6364	-0.0009	5041.0799	0.0032	5005.6211	-0.0048
12	3531.9363	0.0019			3450.6119	-0.0005	5079.0207	-0.0032	5037.2659	0.0019	4998.5950	0.0014
13			3486.0128	0.0010			5078.0871	-0.0023	5033.1348	0.0014	4991.2416	-0.0030
14	3530.7792	-0.0002	3482.0577	-0.0004	3436.4948	0.0054	5076.8353	0.0016	5028.6862	0.0016	4983.5754	-0.0036
15	3529.7733	-0.0010	3477.8245	0.0031	3429.0093	0.0024	5075.2572	0.0007	5023.9165	-0.0012	4975.5963	-0.0006
16	3528.4849	0.0004	3473.3013	-0.0006	3421.2459	0.0017	5073.3542	-0.0032	5018.8344	0.0018	4967.3001	0.0015
17	3526.9103	-0.0001	3468.4972	-0.0021	3413.2048	0.0030	5071.1353	-0.0008	5013.4299	0.0007	4958.6855	0.0016
18	3525.0555	0.0030	3463.4108	-0.0029	3404.8865	0.0060	5068.5961	0.0036	5007.7079	0.0004		
19	3522.9104	-0.0013	3458.0445	-0.0003	3396.2800	-0.0010	5065.7274	0.0013	5001.6653	-0.0019	4940.5033	-0.0035
20			3452.3905	-0.0023	3387.4027	-0.0017			4995.3117	0.0032	4930.9475	0.0031
21	3517.7802	-0.0049			3378.2472	-0.0046			4988.6307	-0.0003	4921.0607	-0.0056
22	3514.8043	0.0022	3440.2432	0.0043	3368.8256	0.0008			4981.6322	-0.0027	4910.8725	-0.0002
23			3433.7352	-0.0018	3359.1149	-0.0100			4974.3199	0.0000	4900.3660	0.0023
24	3507.9881	-0.0175	3426.9505	-0.0013	3349.1504	-0.0038			4966.6814	-0.0046		
25	3504.1946	-0.0019	3419.8841	0.0007	3338.9176	0.0027			4958.7297	-0.0034		
26			3412.5327	0.0012								
27			3404.8865	-0.0100								
28			3396.9792	0.0009					4932.9624	0.0034		
29									4923.7344	0.0055		
30			3380.2932	0.0005					4914.1838	0.0045		
31			3371.5242	-0.0015					4904.3056	-0.0044		
32			3362.4772	0.0012								
33			3353.1498	0.0058								
34			3343.5273	-0.0026								

cm^{-1} on the basis of energy transfer results in the neon matrix experiments. This value compares with 381 ± 100 cm^{-1} predicted by Martin *et al.* (*22*), 0.03 ± 0.02 eV (242 ± 160 cm^{-1}) predicted by Mawhinney *et al.* (*23*), and 181 ± 100 cm^{-1} predicted by Bauschlicher and Partridge (*24*). In the absence of intercombination transitions between the

TABLE 3
Spectroscopic Constants (in cm^{-1}) for the $b^1\Pi - a^1\Sigma^+$ System of ^{11}BN

	$a^1\Sigma^+$			$b^1\Pi$				
Const.[a]	v=0	v=1	v=2	v=0	v=1	v=2	v=3	v=4
T_v	0.0	1684.29646(49)	3347.48617(77)	3513.{9040(43)	5023.47995(42)	6510.78697(47)	7975.95095(74)	9418.92128(76)
B_v	1.6767008(65)	1.6617115(61)	1.6455902(76)	1.5429798(58)	1.5268660(70)	1.5102945(62)	1.4939797(75)	1.4777272(77)
$10^6 \times D_v$	5.9761(89)	6.5207(57)	6.5982(87)	6.3089(45)	6.3557(51)	6.3182(56)	6.3480(86)	6.4820(92)
$10^{10} \times H_v$	-1.453(43)	--	--	--	--	--	--	--
$10^4 \times q_v$	--	--	--	-2.558(28)	0.948(60)	-4.034(25)	-3.634(41)	-3.320(38)
$10^8 \times q_D$	--	--	--	7.03(33)	--	7.11(35)	3.71(86)	-1.33(68)

[a]Numbers in parentheses are one standard deviation in last two digits.

TABLE 4
Spectroscopic Constants (in cm^{-1}) for the $b^1\Pi - a^1\Sigma^+$ System of ^{10}BN

	$a^1\Sigma^+$	$b^1\Pi$	
Const.[a]	v=0	v=0	v=1
T_v	0.0	3511.69964(64)	5062.04186(81)
B_v	1.769962(40)	1.628815(42)	1.610974(41)
$10^6 \times D_v$	6.60(13)	7.30(14)	6.82(14)
$10^{10} \times H_v$	-4.9(13)	4.6(15)	-4.8(14)
$10^4 \times q_v$	--	-1.28(14)	-3.815(25)
$10^7 \times q_D$	--	-7.26(68)	--
$10^9 \times q_H$	--	1.658(83)	

[a]Numbers in parentheses are one standard deviation in last two digits.

singlet and triplet states, it is difficult to determine the precise positions of the singlet states with respect to the ground state. With the exception of the photoelectron spectroscopy of BN^-, the only other method to determine this separation is the observation of perturbations between singlet and triplet states. This method was successfully applied in the case of C_2 where perturbations were observed between the $b^3\Sigma_g^-$ and $X^1\Sigma_g^+$ states (*27*). In the case of BN the only perturbation observed was in the $v = 1$ vibrational level at $J' = 18$ and this was caused by the interaction between the $a^1\Sigma^+$ and $b^1\Pi$ states. This perturbation affects only the *R* and *P* branches indicating that the perturbing state is a $^1\Sigma^+$ state (or more precisely a 0^+ state). The term values indicate that a crossing takes place between the $v = 1$ vibrational level of the $b^1\Pi$ state and the $v = 3$ vibrational level of the $a^1\Sigma^+$ state near $J' = 18$. In the absence of any other perturbation in the $a^1\Sigma^+$ or $b^1\Pi$ states, we are unable to determine the singlet–triplet separation. The observed value of the $T_{00} = 3513.99040(43)$ cm^{-1} for the $b^1\Pi - a^1\Sigma^+$ transition can be compared with the neon matrix value of 3561.6 cm^{-1} of Lorenz *et al.* (*25*) and the ab initio values of 3470 ± 240 cm^{-1} [Mawhinney *et al.* (*23*)] and 3633 cm^{-1} [Bauschlicher and Partridge (*24*)].

The molecular constants of the $a^1\Sigma^+$ and $b^1\Pi$ states have been used to evaluate the equilibrium molecular constants for these states (Table 5). The lower and excited state

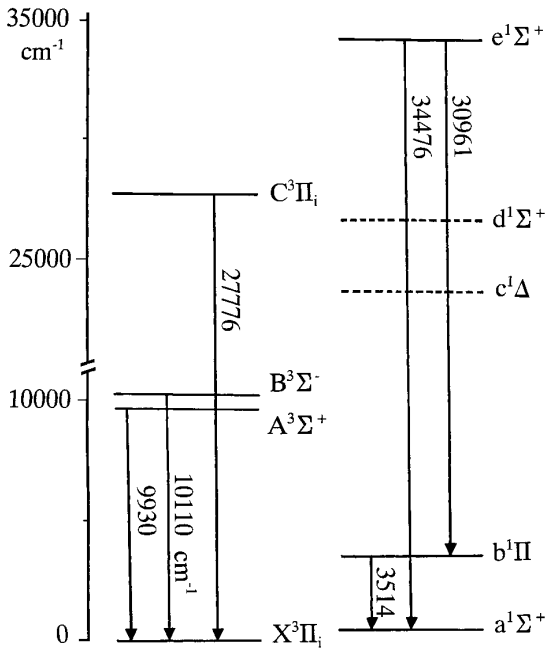

FIG. 3. A schematic energy level diagram of the low-lying electronic states of BN. The positions of the unobserved states (dotted lines) have been taken from the theoretical work of Bauschlicher and Partridge (*24*).

TABLE 5
Equilibrium Constants (in cm^{-1}) for the $a^1\Sigma^+$ and $b^1\Pi$ States of ^{11}BN and ^{10}BN

	^{11}BN		^{10}BN
Const.[a]	$a^1\Sigma^+$	$b^1\Pi$	$b^1\Pi$
ω_e	1705.4032(11)	1531.6526(97)	[1550.3422(10)][b]
$\omega_e x_e$	10.55338(52)	11.0839(20)	--
B_e	1.683771(10)	1.551199(95)	1.637736(52)
α_e	0.013857(16)	0.016335(36)	0.017841(59)
γ_e	-0.0005660(66)	--	--
r_e(Å)	1.2745081(37)	1.327854(41)	1.327805(29)

[a]Numbers in parentheses are one standard deviation in last two digits.
[b]$\Delta G(1/2)$ value.

$\Delta G(1/2)$ vibrational intervals of 1684.29646(49) and 1509.48955(43) cm^{-1} can be compared with the theoretical (*24*) values of 1654.8 and 1476.7 cm^{-1}, as well as the Ne matrix values (*25*) of 1681.1 and 1510.3 cm^{-1}, respectively. The equilibrium rotational constants $B''_e = 1.683771(10)$ cm^{-1} and $B'_e = 1.551199(95)$ cm^{-1} have been used to evaluate the equilibrium bond lengths of 1.2754081(37) and 1.327854(40) Å, respectively, for the $a\,^1\Sigma^+$ and $b\,^1\Pi$ states which can be compared with the most recent theoretical values of Bauschlicher and Partridge (*24*) of 1.286 and 1.341 Å, respectively. These values can also be compared with the experimental value of 1.329 Å in the $X\,^3\Pi$ state. Notice that the bond length of the $a\,^1\Sigma^+$ state is shorter than that of the $X\,^3\Pi$ state even though its $\Delta G(1/2)$ value is larger than that of the $X\,^3\Pi$ state (1514.6 cm^{-1}). The $b\,^1\Pi$ state has a similar bond length and vibrational interval as the $X\,^3\Pi$ state because both of these states come from the same $(2p\pi)^3(2p\sigma)^1$ configuration.

The analysis of the 0–0 and 1–0 bands of the ^{10}BN isotopomer provides a ^{10}BN–^{11}BN isotopic shift of -2.2908 cm^{-1} and $+38.5619$ cm^{-1}, respectively, for these bands. These values can be compared with the corresponding calculated shifts of -2.32 and $+38.64$ cm^{-1} using the vibrational constants of ^{11}BN. The calculated B_e value for the $b\,^1\Pi$ state of ^{10}BN using isotopic relation (*28*) $B_e^i = \rho^2 B_e$ is 1.6387 cm^{-1} which compares well with the observed value of 1.637736(52) cm^{-1} for ^{10}BN.

CONCLUSION

The emission spectrum of BN has been investigated in the infrared region using a Fourier transform spectrometer. The bands observed in the 3000–7900 cm^{-1} region have been assigned to the $b\,^1\Pi$–$a\,^1\Sigma^+$ transition with the 0–0 band at 3514 cm^{-1}. This transition is analogous to the $A\,^1\Pi_u$–$X\,^1\Sigma_g^+$ (Phillips) system of C_2. The rotational analysis of nine bands with $v' = 0$–4 and $v'' = 0$–2 has been obtained and the equilibrium constants for these states have been determined. The present results are consistent with the recent theoretical predictions of Martin *et al.* (*22*) and Bauschlicher and Partridge (*24*) as well as the matrix isolation results of Lorenz *et al.* (*25*).

ACKNOWLEDGMENTS

We thank J. Wagner, C. Plymate, and M. Dulick of the National Solar Observatory for assistance in obtaining the spectra. The National Solar Observatory is operated by the Association of Universities for Research in Astronomy, Inc., under contract with the National Science Foundation. The research described here was supported by funding from the NASA laboratory astrophysics program. Support was also provided by the Natural Sciences and Engineering Research Council of Canada. We thank H. Bredohl for supplying the line positions used in the analysis reported in Ref. (*6*) and C. Bauschlicher for a copy of Ref. (*24*) in advance of publication.

REFERENCES

1. M. Douay, R. Nietmann, and P. F. Bernath, *J. Mol. Spectrosc.* **131,** 250–260 (1988); *J. Mol. Spectrosc.* **131,** 261–271 (1988).
2. K. P. Huber and G. Herzberg, ''Molecular Spectra and Molecular Structure, IV. Constants of Diatomic Molecules,'' Van Nostrand, New York, 1979.
3. A. E. Douglas and G. Herzberg, *Can. J. Res. A* **18,** 179–185 (1940).
4. H. Bredohl, I. Dubois, Y. Houbrechts, and P. Nzohabonayo, *J. Mol. Spectrosc.* **112,** 430–435 (1985).
5. R. D. Verma, *J. Phys. B* **22,** 3689–3694 (1989).
6. H. Bredohl, I. Dubois, Y. Houbrechts, and P. Nzohabonayo, *J. Phys. B* **17,** 95–98 (1984).
7. B. A. Thrush, *Nature* **186,** 1044–1044 (1960).
8. O. A. Mosher and R. P. Frosch, *J. Chem. Phys.* **52,** 5781–5783 (1970).
9. J. L. Masse and M. Bärlocher, *Helv. Chim. Acta* **47,** 314–318 (1964).
10. R. Lefebvre and C. Moser, *C. R. Acad. Sci. (Paris) C* **262,** 901–903 (1966).
11. R. K. Nesbet, *J. Chem. Phys.* **40,** 3619–3633 (1964).
12. G. Verhaegen, W. G. Richards, and C. M. Moser, *J. Chem. Phys.* **46,** 160–164 (1967).
13. P. Sutton, P. Bertoncini, G. Das, T. L. Gilbert, and A. C. Wahl, *Intern. J. Quant. Chem. Ser.* **III,** 479–497 (1970).
14. M. P. Melrose and D. Russell, *J. Chem. Phys.* **55,** 470–471 (1971).
15. R. McWeeny, *Proc. R. Soc. (London) A* **241,** 239–256 (1957).
16. M. P. Melrose and D. Russell, *J. Chem. Phys.* **57,** 2586–2587 (1972).
17. M. F. Guest, I. H. Hillier, V. R. Saunders, and M. H. Wood, *Proc. R. Soc. (London) A* **333,** 201–215 (1973).
18. J. B. Moffat, *J. Mol. Struct.* **16,** 307–309 (1973).
19. S. P. Karna and F. Grein, *Chem. Phys.* **98,** 207–219 (1985).
20. K. Bhanuprakash and R. Buenker, *Chem. Phys. Lett.* **152,** 215–221 (1988).
21. S. P. Karna and F. Grein, *Chem. Phys. Lett.* **144,** 149–152 (1988).
22. J. M. L. Martin, T. J. Lee, G. E. Scuseria, and P. R. Taylor, *J. Chem. Phys.* **97,** 6549–6556 (1992).
23. R. C. Mawhinney, P. J. Bruna, and F. Grein, *Can. J. Chem.* **71,** 1581–1594 (1993).
24. C. W. Bauschlicher Jr., and H. Partridge, *Chem. Phys. Lett.* **257,** 601–608 (1996).
25. M. Lorenz, J. Agreiter, A. M. Smith, and V. E. Bondybey, *J. Chem. Phys.* **104,** 3143–3146 (1996).
26. B. A. Palmer and R. Engleman, ''Atlas of the Thorium Spectrum.'' Los Alamos National Laboratory, Los Alamos, 1983.
27. E. A. Ballik and D. A. Ramsay, *Astrophys. J.* **137,** 84–101 (1963).
28. G. Herzberg, ''Molecular Spectra and Molecular Structure I. Spectra of Diatomic Molecules.'' Van Nostrand, Princeton, 1950.